SEMARAK ILMU PUBLISHING

Journal of Advanced Research in Fluid Mechanics and Thermal Sciences

Journal homepage:
https://semarakilmu.com.my/journals/index.php/fluid_mechanics_thermal_sciences/index
ISSN: 2289-7879

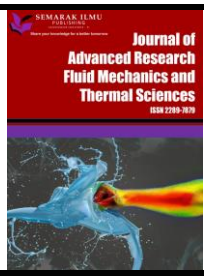

Study on Impact of Magnetic Dipole and Thermal Radiation on Flow/Heat Transfer of Jeffery Fluid over Stretching Sheet with Suction/Injection

Iyoko Michael Ojagabo[1,*], Olajuwon Bakai Ishola[1]

[1] Department of Mathematics, Federal University of Agriculture Abeokuta, P. M. B. 2240 Abeokuta, Ogun State, Nigeria

ARTICLE INFO

Article history:
Received 20 October 2022
Received in revised form 7 February 2023
Accepted 16 February 2023
Available online 9 March 2023

Keywords:
Jeffrey fluid; thermal radiation; stretching sheet; magnetic dipole; prescribed surface temperature; suction/injection

ABSTRACT

In many industries, the knowledge of boundary layer flow and transfer of heat over a stretching sheet is applied. Getting the desired product from these industrial processes is usually a problem. Hence, the purpose of this examination was to establish the impact of thermal radiation and magnetic dipole on the movement and conveyance of heat in Jeffery fluid over a stretching surface that is linear. The model equations of the problem are converted into coupled nonlinear ordinary differential equations employing similarity transformations. The Chebyshev spectral collocation method was utilized to get a solution for the fluid's velocity and temperature. The different parameters in the problem are varied to determine their influence; these effects are represented by tables and graphs as determined by the prescribed surface temperature (PST) and prescribed heat flux (PHF) thermal processes. Results for particular cases are compared with those gotten by the Generic algorithm and Nelder Mead method, and a very good agreement exists. Thermal radiation causes an increment in temperature for PST and PHF processes, while magnetic dipole reduces the velocity of the fluid and increases temperature for the case of PST whereas it exhibits both an increase and decrease in temperature for the PHF case.

1. Introduction

Various industrial and engineering processes like stretching of plasma film, manufacturing of paper and polythene, extrusion of polymer, elastic sheet cooling, growing of crystals, and drawing of wire and fiber technology amongst others usually apply the knowledge of boundary layer flow and heat transfer past a stretching sheet. Hence, there has been continuous interest in the study of fluids flowing over a stretching plate by different researchers. According to Zeeshan and Majeed [1] heat transfer analysis plays an important role because with it the rate of cooling can be easily controlled and the desired properties of the end products could be attained.

Because of this importance, Sakiadis [2] had earlier examined the boundary layer flow over a continuously moving flat surface. A closed-form form analytical solution for two-dimensional incompressible boundary layer flow over a linearly stretching sheet with the distance from the origin

* *Corresponding author.*
E-mail address: mikiyoks@gmail.com

https://doi.org/10.37934/arfmts.104.1.6583

proportional to the velocity was determined by Crane [3]. An extension of this problem was carried out by Gupta and Gupta [4] in which they included heat and mass transfer as well as the effect of suction or blowing. Much other research works on boundary layer flow for the case of Newtonian fluids can be found in the literature [5-11].

Because of the versatility of non-Newtonian fluids, different fluid models under it have been documented extensively in the literature. For example, the Walters' B fluid was considered by different authors in [12-16]. While the Casson Nanofluid was treated by Akaje and Olajuwon [17,19] and Akaje [18]. For this research work, however, our focus is on the Jeffery fluid which is also an example of a non-Newtonian fluid. According to Dalir [20], the model equations of the Jeffery fluid are linear and instead of convected derivatives used for example in the Maxwell fluid model, it utilizes time derivatives. The Jeffery fluid can capture the characteristics of retardation and relaxation times of fluids and its application can be seen in foams, emulsions, slurries, polymers, and solutions amongst others.

The goal of this work is to scrutinize the effect of magnetic field and thermal radiation on the flow of Jeffery fluid over a stretching plate; while considering suction/injection. Hence a look at some research works done on either the MHD flow of Jeffery fluid or the flow of Jeffery fluid in the presence of radiation is presented here. These works include the following and those in the literature. Zeeshan and Majeed [1] analyzed the heat transfer of Jeffery fluid flow over a stretching sheet with suction/injection and magnetic dipole effect; from which they pointed out that the influence of externally applied magnetic field due to the magnetic dipole, causes the fluid velocity to decrease while its temperature increases. Also, they stated that the suction/injection parameter decreases the thermal boundary layer thickness. An MHD stagnation point flow of Jeffery fluid by a radially stretching surface with viscous dissipation and joule heating was considered by Hayat *et al.,* [21]. The stagnation point flow of MHD Jeffrey Nanofluid over a stretching surface with an induced magnetic field and the chemical reaction was carried out by Sandeep *et al.,* [22]. Hayat and Mustafa [23] verified the influence of thermal radiation on the unsteady mixed convection flow of a Jeffery fluid over a stretching sheet. An analysis of the effects of nonlinear thermal radiation on 3D Jeffrey fluid flow over a stretching/shrinking surface in the presence of homogeneous-heterogeneous reactions, non-uniform heat source/sink, and suction/injection was done by Raju *et al.,* [24]. The work of Hayat *et al.,* [25] studied a Jeffery fluid flow in a porous channel in the presence of a transverse magnetic field. The homotopy analysis method (HAM) was used to find a semi-analytical solution to the highly nonlinear model equations. A study of the motion of viscoelastic fluid toward a stretching sheet in the presence of an induced magnetic field for the case of unequal diffusivities of homogeneous–heterogeneous reaction with thermal radiation was performed by Animasaun *et al.,* [26]; it was discovered that the nonlinear thermal radiation improves the temperature profiles and suppresses the rate of heat transfer. Narayana and Babu [9] carried out a numerical study of MHD heat and mass transfer of a Jeffery fluid over a stretching sheet with chemical reaction and thermal radiation. The research paper of Shehzad *et al.,* [27], investigated nonlinear thermal radiation in the three-dimensional flow of Jeffery Nanofluid: A model for solar energy. Das *et al.,* [28] carried out the analysis of the radiative flow of MHD Jeffery fluid past a stretching sheet with surface slip and melting heat transfer, while Dalir *et al.,* [29] performed the entropy analysis for magnetohydrodynamic flow and heat transfer of a Jeffery Nanofluid over a stretching sheet. Also, Hayat *et al.,* [30] considered the MHD flow of Jeffery liquid due to a nonlinear radially stretched sheet in presence of Newtonian heating. The flow of micropolar ferromagnetic fluid due to the stretching of an elastic sheet in the presence of an applied magnetic field was examined by Narayana *et al.,* [31].

For these works cited above, it was observed that the magnetic field effect results in the reduction of the flow velocity and increment in its temperature. While thermal radiation usually increases the

fluid temperature. Only a few of these works were able to consider both magnetic field effect and thermal radiation, hence the need for this research work as it would consider both magnetic dipole and thermal radiation effect on the Jeffery fluid flow over a stretching plate; as these processes could occur simultaneously in industrial applications.

Some latest works include those of Khan *et al.,* [39] that studied the MHD flow and heat transfer of double stratified micropolar fluid over a vertical permeable shrinking/stretching sheet with chemical reaction and heat source. Considering the presence of suction, it was discovered that the skin friction coefficient and the local Nusselt number increase with increasing heat source parameters. Also, the heat source parameter tends to decrease the magnitude of the local Sherwood number. This present work is also considering suction/injection as the fluid flows over the stretching sheet.

Rehman *et al*., [40] considered a three-dimensional incompressible MHD flow of a micropolar carbon-water nanofluid in the presence of a rotating frame, where it was observed that the temperature profile decreases with the increase in porosity parameter and nanoparticle volume fraction while Micro rotation profile increases with the increase in coupling parameter and Reynolds number.

Salient aspects of entropy generation optimization in mixed convection nanomaterial flow were studied by Ijaz Khan *et al.,* [41] and it shows that increasing the magnetic parameter decreases the velocity and increases the temperature profile.

Rusdi *et al.,* [42] examined thermal radiation in Nanofluid penetrable flow bounded with partial slip condition, and found that increment in the suction parameter led to a decrease in the temperature profile. Besides that, the skin friction coefficient and Nusselt number increase when the suction parameter increases.

In the work by Kotnurkar and Kallolikar [43], the electro-osmosis peristaltic flow of Eyring Powell nanofluid in a tapered asymmetric channel was analyzed and it was observed that with an increase in the Hartmann number the velocity profile decreases.

This paper shall extend the work of Zeeshan and Majeed [1] to include thermal radiation and use the Chebyshev Spectral Collocation Method to obtain results for the velocity and temperature of the Jeffery fluid flowing past a stretching sheet, providing a detailed analysis of the influence of thermal radiation and a magnetic dipole.

2. Methodology

2.1 Magnetic Dipole

According to Zeeshan and Majeed [1], the dipole field with permanent magnetic scalar potential (φ) usually affects the flow of a magnetic fluid. We write φ as

$$\varphi = \frac{\gamma}{2\pi}\left(\frac{x}{x^2+(y+a)^2}\right) \tag{1}$$

Given that γ is the magnetic field's strength. The magnetic field has intensities along the x and y axes denoted by H_x and H_y respectively. They are given as

$$H_x = -\frac{\partial \varphi}{\partial x} = \frac{\gamma}{2\pi}\left(\frac{x^2-(y+a)^2}{(x^2+(y+a)^2)^2}\right) \tag{2}$$

$$H_y = -\frac{\partial \varphi}{\partial y} = \frac{\gamma}{2\pi}\left(\frac{2x(y+a)}{(x^2+(y+a)^2)^2}\right) \tag{3}$$

The resultant magnitude H of these intensities is written as

$$H = \left[\left(\frac{\partial \varphi}{\partial x}\right)^2 + \left(\frac{\partial \varphi}{\partial y}\right)^2\right]^{\frac{1}{2}} \tag{4}$$

$$\frac{\partial H}{\partial x} = -\frac{\gamma}{2\pi}\left(\frac{2x}{(y+a)^4}\right) \tag{5}$$

$$\frac{\partial H}{\partial y} = \frac{\gamma}{2\pi}\left(\frac{-2}{(y+a)^3} + \frac{4x^2}{(y+a)^5}\right) \tag{6}$$

According to Andersson and Valnes [32], the variation of magnetization M can be regarded as a linear function of temperature and given as

$$M = K^*(T_c - T) \tag{7}$$

where K^* is referred to as the pyromagnetic coefficient and T_c is called the Curie temperature; however, for there to exist ferrohydrodynamic interaction the following is important

i. the fluid is at a temperature T different from T_c, and
ii. the external magnetic field is inhomogeneous.

Titus and Abraham [33] cited that, immediately after the ferromagnetic fluid reaches Curie temperature, magnetization no longer occurs. Characteristics for physical significance is very essential, since Curie temperature is very high, that is 1043 K for iron.

2.2 Analysis of the Flow

We consider a Jeffrey fluid flow in two dimensions, over a stretching sheet that is affected by the magnetic field caused by a magnetic dipole. The fluid is regarded as one that does not conduct electricity. The stretching plate is along the x-axis and has velocity $u_w = cx$ while the y-axis is perpendicular to it. Figure 1 shows the schematics of the problem. In the middle of the y-axis, a magnetic dipole is placed a distance ‘‘a” from the stretching plate. Because of the dipole, the direction of the magnetic field is the positive x-direction and the strength of the magnetic field is increased so that the ferrofluid becomes more tender or marinated. Also, it is assumed that the steady temperature at the surface is T_w and less than the Curie temperature T_c, whereas the temperature of the surrounding ferrofluid far from the sheet’s surface is $T_\infty = T_c$ and this ambient fluid is not able to magnetize until they begin to cool after reaching the thermal boundary layer area near the sheet.

Some of the physical situations that is being modelled in this work include these physical applications of Ferrofluid mentioned below. Ferrofluids have found a use in non-destructive testing of components containing hollow inner features. This is simply because they are liquids and because they are magnetic. Many modems non-magnetic components are made with cooling gas channels, oilways, or cavities within them. The inner hollows can be filled with ferrofluid and the presence of the magnetic liquid can be detected from the outside of the component with a probe sensitive to permeability changes. The ferrofluid can then be washed out of the component. The magnitude of the signal from the probe is strongly related to the volume of ferrofluid beneath the surface, the

distance from the probe to the ferrofluid, and the saturation magnetisation value of the ferrofluid. Also, the viscous damping available from ferrofluid is useful in a general range of measuring instruments (for example, a flow meter and an ink viscometer). The unique advantage of ferrofluid is that it does not need a closed vessel with its attendant sealing problems to contain the liquid. The magnetic liquid can be held in position with a simple permanent magnet regardless of the orientation of the device relative to gravity or motion [44].

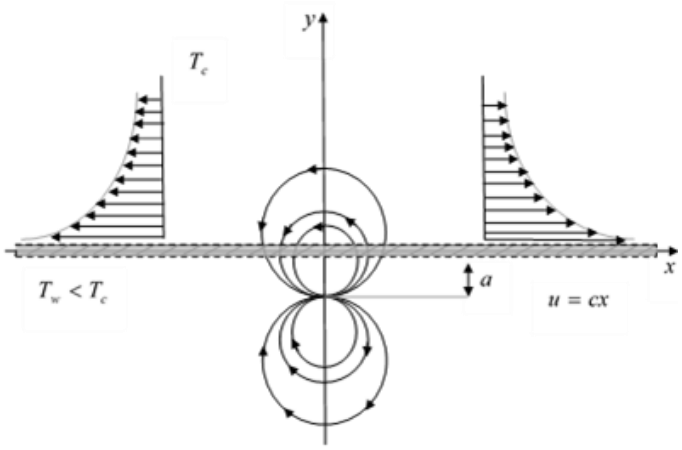

Fig. 1. Schematic of the problem with circles representing magnetic dipole

As can be found in Nadeem and Akbar [34], the model equation of Jeffrey fluid is given as

$$\tau = -pI + \kappa \tag{8}$$

$$\kappa = \frac{\mu}{1+\lambda_2}\left[A_1 + \lambda_1\left(\frac{\partial A_1}{\partial t} + \boldsymbol{V}\cdot\nabla A_1\right)\right] \tag{9}$$

where τ is the Cauchy stress tensor, the extra stress tensor is κ, the dynamic viscosity is μ, the material parameters of Jeffery fluid are λ_1 and λ_2, while A_1 is the first Rivlin-Ericksen tensor written as

$$A_1 = (\nabla \boldsymbol{V}) + (\nabla \boldsymbol{V})^T \tag{10}$$

With the use of boundary layer approximations, we get the equations for continuity and momentum of Jeffery fluid as

$$\frac{\partial u}{\partial x} + \frac{\partial v}{\partial y} = 0 \tag{11}$$

$$u\frac{\partial u}{\partial x} + v\frac{\partial u}{\partial y} = \frac{\mu_0}{\rho}M\frac{\partial H}{\partial x} + \frac{\nu}{1+\lambda_2}\left[\frac{\partial^2 u}{\partial y^2} + \lambda_1\left(u\frac{\partial^3 u}{\partial x \partial y^2} + v\frac{\partial^3 u}{\partial y^3} - \frac{\partial u}{\partial x}\frac{\partial^2 u}{\partial y^2} + \frac{\partial u}{\partial y}\frac{\partial^2 u}{\partial x \partial y}\right)\right] \tag{12}$$

where the components of velocity in the x and y direction are respectively u and v. The relaxation time is λ_1 while the ratio of relaxation to the retardation times is λ_2, the fluid's density is ρ, ν is the kinematic viscosity, the magnetic permeability is μ_0, also k, c_p, M and H are the thermal conductivity, specific heat, magnetization, and the magnetic field intensity respectively.

The boundary conditions required for the velocity profile as given in Zeeshan and Majeed [1] are

$$u = u_w = cx, \qquad v = v_w, \qquad \text{at } y = 0$$
$$u \to 0, \qquad \frac{\partial u}{\partial y} \to 0, \qquad \text{as} \quad y \to \infty \tag{13}$$

where $c > 0$ is the rate of stretching of the sheet, and v_w is the suction/injection velocity.

These similarity transformations as gotten from Andersson and Valnes [32] as well as Dalir [20] are used in Eq. (12)

$$\psi(\xi, \eta) = \left(\frac{\mu}{\rho}\right) \xi \cdot f(\eta), \; \xi = \sqrt{\frac{c\rho}{\mu}} x, \;\; \eta = \sqrt{\frac{c\rho}{\mu}} y \tag{14}$$

The stream function is $\psi(\xi, \eta)$ and the non-dimensional coordinates are ξ, η. The velocity components are derived as

$$u = \frac{\partial \psi}{\partial y} = cx \cdot f'(\eta), v = -\frac{\partial \psi}{\partial x} = \sqrt{cv} \cdot f(\eta) \tag{15}$$

When we put Eq. (15) into Eq. (12) and compare coefficients of similar powers up to ξ^2, we shall arrive at the following nonlinear differential equation which is of fourth order

$$f'' - (1 + \lambda_2)\left(f'^2 - ff''\right) + \gamma_1\left(f''^2 - ff^{iv}\right) - (1 + \lambda_2)\frac{2\beta\theta_1}{(\eta + \alpha_1)^4} = 0 \tag{16}$$

Applying the transformations to Eq. (13) we get the dimensionless boundary conditions

$$f = \mathrm{S}, \; f' = 1, \quad \text{at } \eta = 0$$
$$f' \to 0, \qquad f'' \to 0, \qquad \text{as} \quad \eta \to \infty \tag{17}$$

Such that $\gamma_1 = \lambda_1 c$ is regarded as the Deborah number and the ferromagnetic interaction parameter is

$$\beta = \frac{\gamma\rho}{2\pi\mu^2} \mu_0 K^* (T_c - T_w),$$

while the suction/injection parameter is given as $\mathrm{S} = \frac{-v_w}{\sqrt{cv}}$ with $\mathrm{S} > 0$ meaning suction and $\mathrm{S} < 0$ meaning injection.

2.3 Transfer of Heat

Incorporating thermal radiation into the energy equation of Titus and Abraham [33] we have

$$\rho c_p \left(u\frac{\partial T}{\partial x} + v\frac{\partial T}{\partial y}\right) + \mu_0 T \frac{\partial M}{\partial T}\left(u\frac{\partial H}{\partial x} + v\frac{\partial H}{\partial y}\right) = \mathrm{k}\frac{\partial^2 T}{\partial y^2} + \mu\left(\frac{\partial u}{\partial y}\right)^2 + 2\mu\left(\frac{\partial v}{\partial y}\right)^2 - \frac{\partial q_r}{\partial y} \tag{18}$$

where c_p is the specific heat, T is the temperature of the fluid, k is the thermal conductivity and q_r is radiative heat flux. The contribution this research work can make to the existing literature is the fact that the existing literature had not considered the impact of thermal radiation on the flow a

ferrofluid over a stretching sheet with magnetic dipole effect and suction/injection. The findings from this work therefore, would enable researchers and engineers know how to best handle the heat and mass transfer of this fluid in the various physical applications mentioned above.

The non-isothermal temperature boundary condition required to solve Eq. (17) is given by Zeeshan and Majeed [1] as

$$\left.\begin{aligned} T = T_w = T_c - A\left(\frac{x}{l}\right)^2 \qquad & for\ PST \\ q_w = -k\frac{\partial T}{\partial y} = D\left(\frac{x}{l}\right)^2 \qquad & for\ PHF \end{aligned}\right\} \qquad at \quad y = 0$$

$$T \to T_c \qquad as \quad y \to \infty \tag{19}$$

where A and D are positive constants and $l = \sqrt{\nu/c}$ is the characteristic length.

According to Narayana and Babu [9], as well as Raptis [35], we can use the Rosseland diffusion approximation to get the radiative heat flux, q_r as

$$q_r = -\frac{4\sigma^*}{3K_s}\frac{\partial T^4}{\partial y} \tag{20}$$

where σ^* is the Stefan-Boltzmann constant and $K_s$is the Rosseland mean absorption coefficient. Assuming that the differences in temperature inside the flow are sufficiently small such that T^4 may be given as a linear function of temperature.

$$T^4 \approx 4T_c^4 T - 3T_c^4 \tag{21}$$

Hence, we have the last term in Eq. (18) given as

$$\frac{\partial q_r}{\partial y} = -\frac{16\sigma^* T_c^3}{3K_s}\frac{\partial^2 T}{\partial y^2} \tag{22}$$

With the introduction of the non-dimensional variable $\theta(\xi, \eta)$

$$\theta(\xi, \eta) \equiv \frac{T_c - T}{T_c - T_w} = \theta_1(\eta) + \xi^2\theta_2(\eta) \tag{23}$$

where

$$T_c - T_w = A\left(\frac{x}{l}\right)^2 \quad for\ PST, \quad T_c - T_w = \frac{D}{k}\left(\frac{x}{l}\right)^2\sqrt{\frac{\nu}{c}} \quad for\ PHF.$$

The dimensionless energy equations up to order ξ^2 are derived when we put Eq. (22) in Eq. (18) as

$$\left(1 + \frac{4}{3}R_d\right)\theta_1'' + \Pr(f\theta_1' - 2f'\theta_1) + \frac{2\lambda\beta(\theta_1 - \varepsilon)f}{(\eta+\alpha_1)^3} - 2\lambda f'^2 = 0 \tag{24}$$

$$\left(1 + \frac{4}{3}R_d\right)\theta_2'' + \Pr(4f\theta_2' - 2f'\theta_2) + \frac{2\lambda\beta\theta_2 f}{(\eta+\alpha_1)^3} - \lambda\beta(\theta_1 - \varepsilon)\left[\frac{2f'}{(\eta+\alpha_1)^4} + \frac{4f}{(\eta+\alpha_1)^5}\right] - \lambda f'^2 = 0 \tag{25}$$

Where the Prandtl number is given as $Pr = \frac{\mu c_p}{k}$, the viscous dissipation parameter is $\lambda = \frac{c\,\mu^2}{\rho k(T_c - T_w)}$, non-dimensional Curie temperature ratio is $\varepsilon = \frac{T_c}{T_c - T_w}$, and the non-dimensional distance from the origin to the magnetic dipole is $\alpha_1 = \sqrt{\frac{c\,\rho}{\mu}}\,a$.

We now have the thermal boundary conditions as

$$\left.\begin{array}{ll} \theta_1 = 1, & \theta_2 = 0\,, \quad for\ PST \\ \theta_1' = -1, & \theta_2' = -1\,, \quad for\ PHF \end{array}\right\} \qquad at \quad \eta = 0$$

$$\theta_1 \to 0, \quad \theta_2 \to 0 \qquad as \quad \eta \to \infty \tag{26}$$

The local skin-friction coefficient and the local Nusselt number are quantities that are of great importance physically, they are written as

$$C_{fx} \equiv \frac{-2\,\tau_w}{\rho\,(cx)^2}\,,\ Nu_x \equiv \frac{x\,q_w}{-k\,(T_c - T_w)^2} \tag{27}$$

where τ_w, the surface shear stress, and q_w, the surface heat flux is given as

$$\tau_w = \mu\left(\frac{\partial u}{\partial y}\right)_{y=0}, \quad q_w = -\left(\frac{\partial T}{\partial y}\right)_{y=0} \tag{28}$$

Employing Eq. (15) and Eq. (23) on Eq. (27) leads us to

$$\left.\begin{array}{rl} C_f\,Re_x^{\frac{1}{2}} = -2\,f''(0), & \\ Nu_x\,Re_x^{-\frac{1}{2}} = -\left(1+\frac{4}{3}R_d\right)\left(\theta_1'(0) + \xi^2\theta_2'(0)\right) & for\ PST \\ Nu_x\,Re_x^{-\frac{1}{2}} = 1/\left(1+\frac{4}{3}R_d\right)\left(\theta_1'(0) + \xi^2\theta_2'(0)\right) & for\ PHF \end{array}\right\} \tag{29}$$

where the local Reynolds number is given as

$$Re_x = \frac{\rho\,cx^2}{\mu}.$$

The flow is affected by the ferromagnetic parameter β. It is more captivating and fitting to replace the non-dimensional wall heat transfer rate $-\theta' = \left(\theta_1'(0) + \xi^2\theta_2'(0)\right)$ by the term independent of the distance ξ, called the coefficient of the heat transfer rate at the plate; which is given by the ratio

$$\theta^*(0) = \frac{\theta_1'(0)}{\theta_1'(0)|_{\beta=0}}.$$

2.4 Calculation

The Chebyshev Spectral Collocation Method (CSCM) is applied to solve the nonlinear momentum and energy Eq. (16) and Eq. (24) together with the boundary conditions (17) and (26). Here, the unknown velocity and temperature functions, $f(\eta)$ and $\theta(\eta)$ are approximated by the sum of the basis function $T_n(\eta)$ as seen in Akaje and Olajuwon [17], that is

$$f(\eta) = \sum_{n=0}^{N} a_n \, T_n(\eta) \tag{30}$$

$$\theta(\eta) = \sum_{n=0}^{N} b_n \, T_n(\eta) \tag{31}$$

This basis function used in the method is the Chebyshev polynomial N defined on the closed interval $[-1,\ 1]$ and given as

$$T_n(\eta) = \cos\left(\mathrm{N}\cos^{-1}\bar{\eta}\right) \tag{32}$$

Collocation points (the Gauss-Lobatto set) given as in Pruett and Streett [36] as well as Sobamowo *et al.,* [37]

$$\bar{\eta} = \cos\left(\frac{\pi\, j}{N}\right), \qquad j = 0, 1, 2, \dots, N \tag{33}$$

are used to discretize the interval $[-1, 1]$ and to define the Chebyshev nodes inside.

The unknown constants to be obtained are a_n and b_n. The unbounded domain of problem $[0, \infty]$, is transformed into the $[-1, 1]$ of the definition of the basis function, by utilizing the transformation below

$$\eta = \frac{2\,\xi}{\xi_\infty - 1} \tag{34}$$

where the boundary layer at the extreme edge of the stretching sheet is denoted by ξ_∞.

Eq. (30) and Eq. (31) are substituted in (16) and (24) to derive non-zero residuals, and the constants a_n and $b_n$are determined in such a way that there is a minimization of the residuals all through the domain.

3. Results

Implementing the Chebyshev Spectral Collocation Method (CSCM) above in Mathematica, we varied the various parameters in the model to determine their impact on the velocity and temperature of the Jeffrey fluid over the stretching surface. The following values for the parameters were taken as their automatic values whenever they are not being varied; $\beta = 0.2, \lambda = 0.02, \lambda_2 = 0.1, \gamma_1 = 0.2, \mathrm{S} = 0.1, \mathrm{Pr} = 1.0, \mathrm{R_d} = 1.0, \alpha_1 = 1.0, \varepsilon = 2$ to verify the efficiency of the Chebyshev Spectral Collocation Method (CSCM) used in this work, we computed results for $-\theta_1{}'$ taking various values of Pr and compared with what was gotten by Abel *et al.,* [38] and Zeeshan and Majeed [1]. As can be seen in Table 1, there is an excellent consensus.

Table 1
Comparison of Nusselt number $-\theta_1{}'$ for the case $\beta = \ \lambda = \lambda_2 = \gamma_1 = \mathrm{S} = 0.1, \mathrm{R_d} = 1.0$

Pr	Abel *et al.,* [38]	Zeeshan and Majeed [1]	Current result
0.72	1.0885	1.088527	1.0885252
1	1.3333	1.333333	1.3333333
3	–	2.509725	2.5097266
10	4.7968	4.796873	4.7956998

In Table 2, we present the skin friction coefficient $-f''(0)$ and Nusselt number $-\theta_1'(0)$ values for the prescribed surface temperature (PST) case and temperature function $\theta_1(0)$ values for the prescribed heat flux (PHF) case as derived for the Generic Algorithm and Nelder-Mead (GA and NM) solution of Zeeshan and Majeed [1] and those determined using the Chebyshev Spectral Collocation Method (CSCM). From the solutions of the CSCM, it is clear that for the PST case the Nusselt number increases as the Prandtl number increases but it reduces as the Deborah number, ferromagnetic interaction parameter, suction/injection parameter as well as the ratio of relaxation and retardation times all increases. The Skin friction coefficient and the surface temperature for PHF case increases as the ferromagnetic interaction parameter together with the ratio of relaxation and retardation increases. Increase in Prandtl number and Deborah number cause reduction in the skin friction coefficient. Whereas increasing Deborah number increases the surface temperature; increasing Prandtl number reduces the surface temperature. The only variation with the solution of GA and NM is that increase in Deborah number and suction/injection parameter increases Nusselt number, while increase in increase in Deborah number reduces surface temperature.

Table 2
Skin friction coefficient $-f''(0)$, Nusselt number $-\theta_1'(0)$ and temperature function $\theta_1(0)$ for various values of $\beta, \lambda, \lambda_2, \gamma_1, \mathrm{S}$ and Pr when $\mathrm{R_d} = 0$

Pr	β	λ_2	γ_1	S	λ	Series solution based on GA and NM Zeeshan and Majeed [1]			Solution based on CSCM		
						$-f''(0)$	PST $-\theta_1'(0)$	PHF $\theta_1(0)$	$-f''(0)$	PST $-\theta_1'(0)$	PHF $\theta_1(0)$
1.0	0.2	0.1	0.2	0.1	0.01	1.0470	1.3958	0.7138	1.0523	1.3954	0.7142
2.0						1.0399	2.1184	0.4697	1.0000	2.0000	0.5000
3.0						1.0357	2.6848	0.3705	1.0000	2.5097	0.3985
3.0	2.0	0.1	0.2	0.1	0.01	1.3986	2.6458	0.3706	1.4411	2.6406	0.3710
	3.0					1.6042	2.6223	0.3705	2.3730	0.0908	2.3629
	4.0					1.8131	2.5973	0.3708	2.8094	0.1762	1.9841
3.0	0.2	0.1	0.2	0.1	0.01	1.0355	2.6848	0.3704	1.0397	2.6845	0.3707
		0.2				1.0814	2.6728	0.3722	1.0954	0.0526	18.9465
		0.3				1.1255	2.6613	0.3739	1.1402	0.0526	18.9963
3.0	0.2	0.1	0.1	0.1	0.01	1.0914	2.6710	0.3724	1.0962	2.6705	0.3726
			0.2			1.0354	2.6849	0.3705	0.9129	0.0527	18.9274
			0.3			0.9875	2.6967	0.3689	0.8771	0.0527	18.9930
3.0	0.2	0.1	0.2	0.1	0.01	1.0355	2.6848	0.3704	1.0397	2.6845	0.3707
				0.4		1.1377	3.2293	0.3079	1.2198	0.0527	18.9527
				0.6		1.2060	3.6325	0.2739	1.3440	0.0526	18.9974
3.0	0.2	0.1	0.2	0.1	0.4	1.0335	2.9106	0.2848	1.0376	2.9103	0.2849
					0.6	1.0325	3.0268	0.2405	1.0000	0.6369	7.5325
					0.8	1.0316	3.1432	0.1961	1.0000	0.8316	4.0208

The ferromagnetic interaction parameter β depicts the effect of the external magnetic field that is applied to the system as a result of a magnetic dipole. The presence of magnetic field functions as a force that pulls back velocity, so as β becomes higher the force that delays velocity also increases, and hence the velocity in the axial direction $f'(\eta)$ becomes flattened. All of this is because changes in the magnetic parameter bring about a deviation of Lorentz force and this force creates extra

resistance to the phenomena of transport. Figure 2(a) and Figure 2(b) show the velocity profile for the PST and PHF cases respectively and we see that as the ferromagnetic interaction parameter increases beyond the hydrodynamic point ($\beta = 0$) the velocity reduces for both cases. The velocity becomes lesser because there is an interference between the action of the magnetic field applied and the motion of the fluid, this interference also makes the frictional heating inside the layers of the fluid to be increased as we can visibly see in Figure 3(a) that the temperature profile increases for PST. For the PHF case in Figure 3(b) we see that the temperature profile increases as β value increase from zero to two ($\beta = 0$ to $\beta = 2$)– for lesser values $\beta = 0, 0.5, 1, 2$ we have a steady increase in temperature profile, but for higher values of β there is a fall in temperature. This behavior of the temperature profile for the PHF case is most likely because of the presence of thermal radiation interfering with the magnetic dipole.

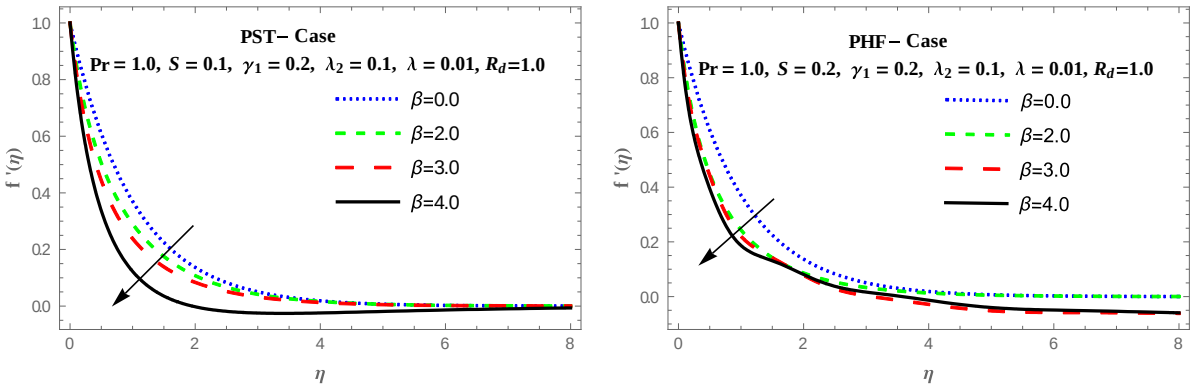

(a) (b)

Fig. 2. Influence of ferromagnetic interaction parameter β on velocity $f'(\eta)$: (a) for PST and (b) for PHF

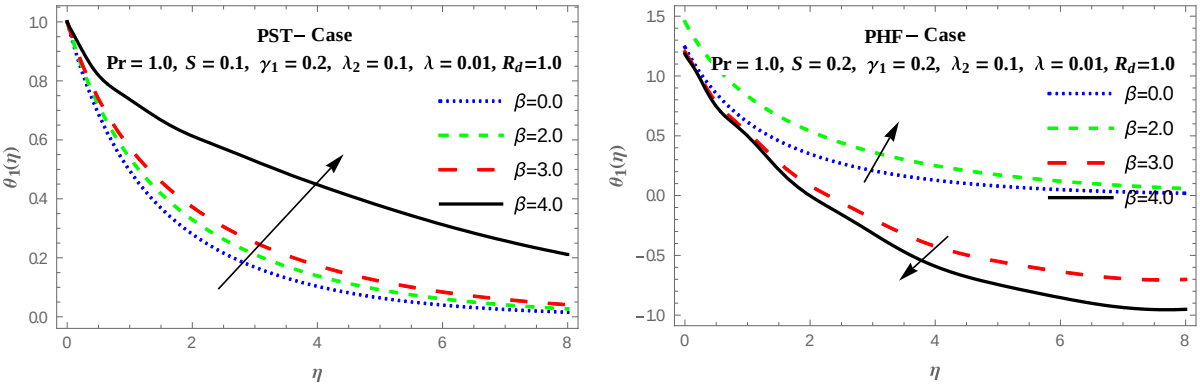

(a) (b)

Fig. 3. Influence of ferromagnetic interaction parameter β on temperature θ_1: (a) for PST and (b) for PHF

The effect of Deborah number (γ_1) on velocity for both the PST and PHF cases is presented in Figure 4(a) and Figure 4(b), where we see that γ_1 enhances the velocity profile as it increases. The influence on the temperature for both types of thermal processes by the Deborah number is shown in Figure 5(a) and Figure 5(b). As γ_1 increases there is a reduction in the temperature θ_1 for PST and PHF cases. Deborah number is physically proportional to retardation time λ_1; therefore, when any material has a large retardation time its viscosity is lesser, which causes its motion to increase, and ultimately the thermal boundary layer thickness is weakened leading to a lower profile for the temperature.

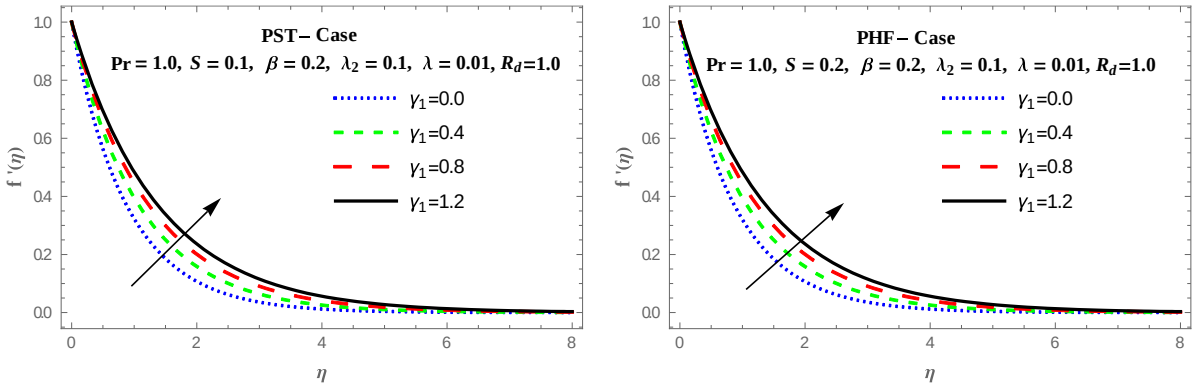

(a) (b)

Fig. 4. Influence of Deborah number γ_1 on velocity $f'(\eta)$: (a) for PST and (b) for PHF

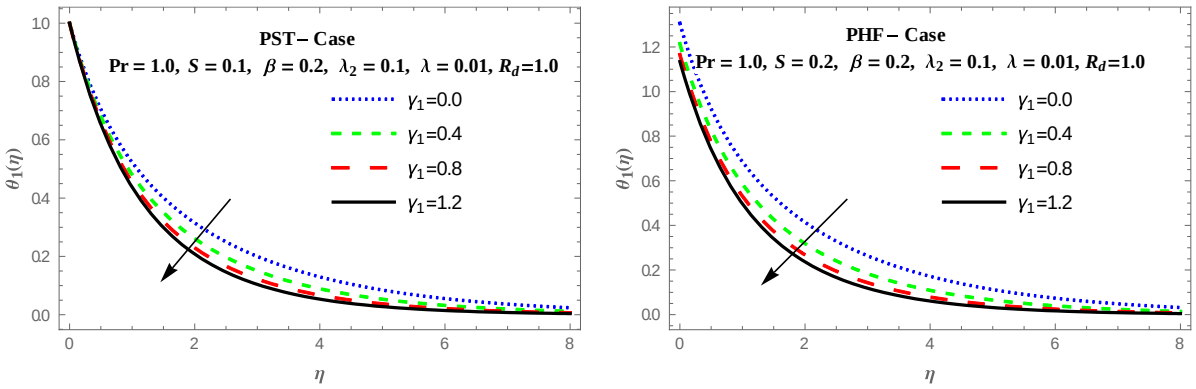

(a) (b)

Fig. 5. Influence of Deborah number γ_1 on temperature θ_1: (a) for PST and (b) for PHF

The influence of the ratio of relaxation to retardation time parameter λ_2 on the velocity for PST and PHF cases is depicted in Figure 6(a) and Figure 6(b) respectively. It reveals that as λ_2 values become larger the velocity profile diminishes. In Figure 7(a) and Figure 7(b) we have the behavior of temperature as affected by the ratio of relaxation to retardation timeλ_2, these figures show a steady rise in temperature profile with an increase in the value of λ_2. When λ_2 increases it means that the retardation time reduces while the relaxation increases, this change explains the increase in thermal boundary layer thickness and temperature.

The behavior of velocity as the suction/injection parameter S changes is portrayed in Figure 8(a) and Figure 8(b) for the PST and PHF cases. We see that increase in S causes a gradual decrease in the velocity profile of the fluid. Figure 9(a) and Figure 9(b) show the effect of suction/injection on the temperature for thermal processes PST and PHF. The injection is represented by negative values of S, whereas positive values mean suction. Although there is a general reduction in the temperature profile for both PST and PHF cases, we notice from the figures that the reduction is very small for $S < 0$ but there is a larger reduction for $S > 0$.

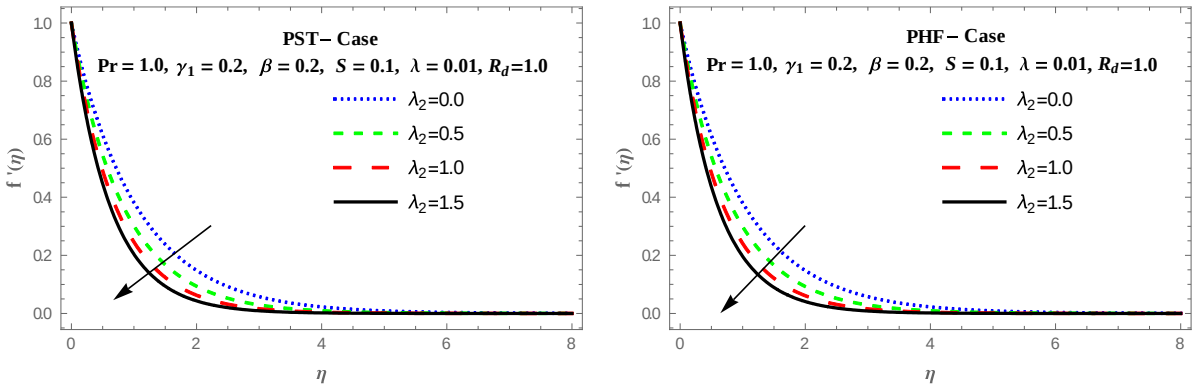

(a) (b)

Fig. 6. Influence of the Ratio of relaxation to retardation time λ_2 on velocity $f'(\eta)$: (a) for PST and (b) for PHF

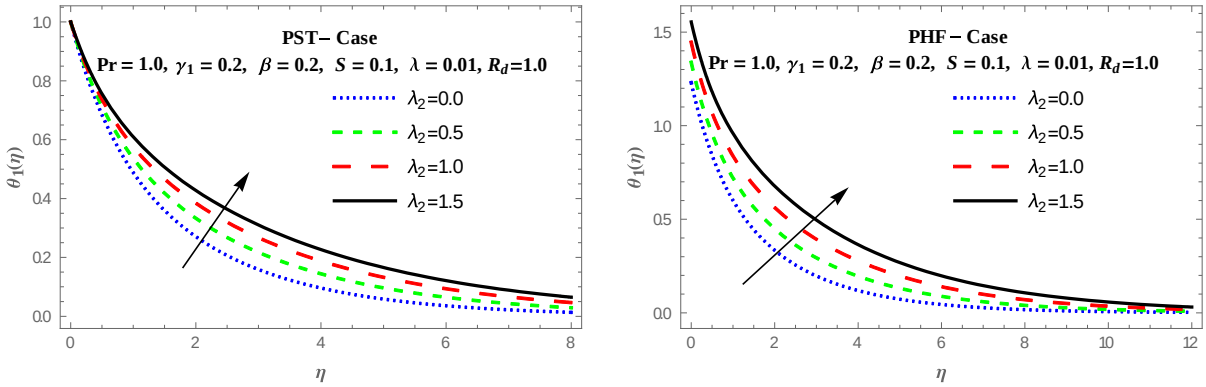

(a) (b)

Fig. 7. Influence of the Ratio of relaxation to retardation time λ_2 on temperature θ_1: (a) for PST and (b) for PHF

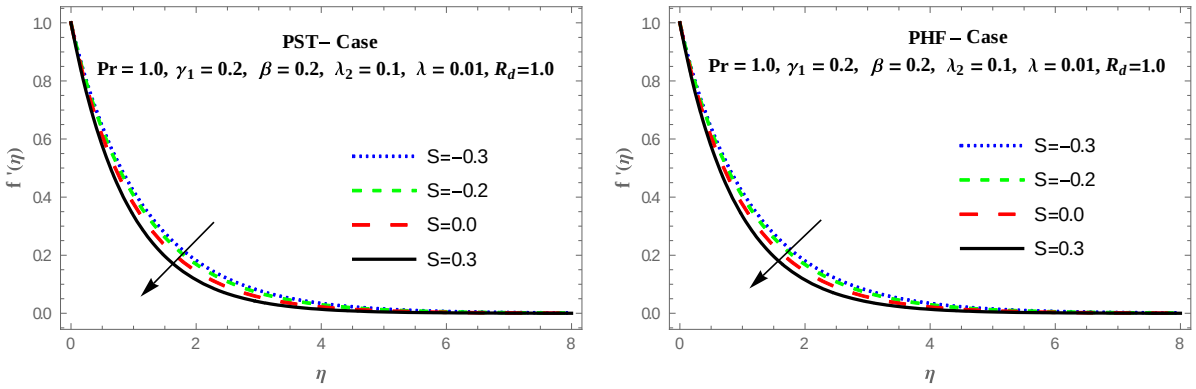

(a) (b)

Fig. 8. Influence of suction/injection S on velocity $f'(\eta)$: (a) for PST and (b) for PHF

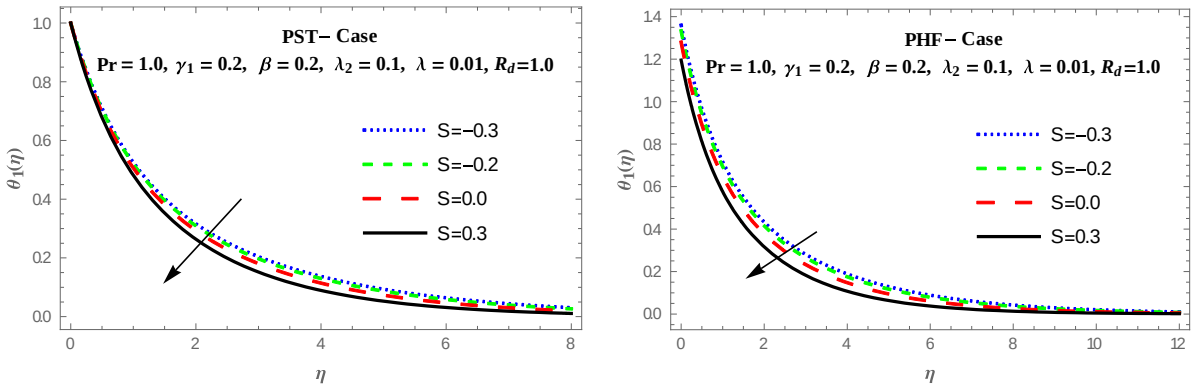

(a) (b)

Fig. 9. Influence of suction/injection S on temperature θ_1 : (a) for PST and (b) for PHF

From the velocity profile in Figure 10(a) and Figure 10(b) which are for both the PST and PHF cases, we see that increasing the value of the Prandtl number Pr does not show any significant change in the velocity of the system. The effect of the Prandtl number on the temperature for both thermal processes PST and PHF is delineated in Figure 11(a) and Figure 11(b). The rise in Pr leads to decrement in the temperature profile. This happens because when we have higher values of the Prandtl number the thermal conductivity of the fluid is quite smaller, hence thermal boundary layer thickness and conduction experience a reduction and we have the temperature decrease.

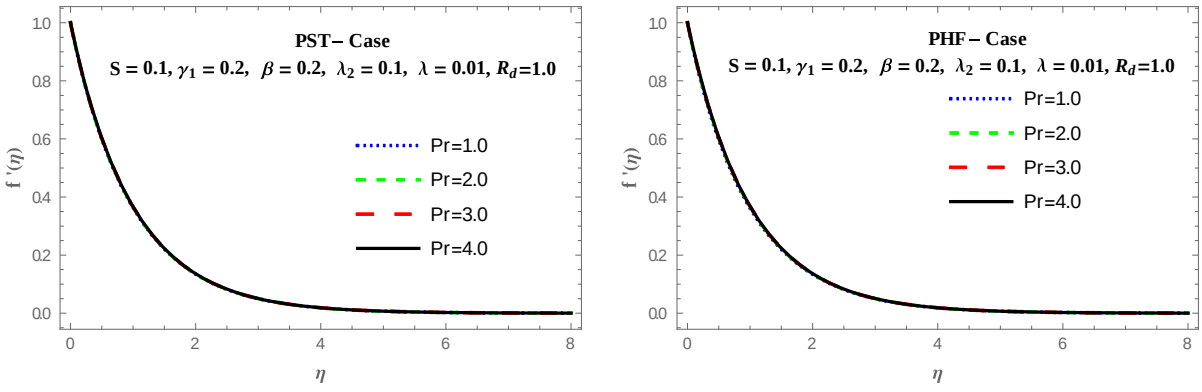

(a) (b)

Fig. 10. Influence of Prandtl number Pr on velocity $f'(\eta)$: (a) for PST and (b) for PHF

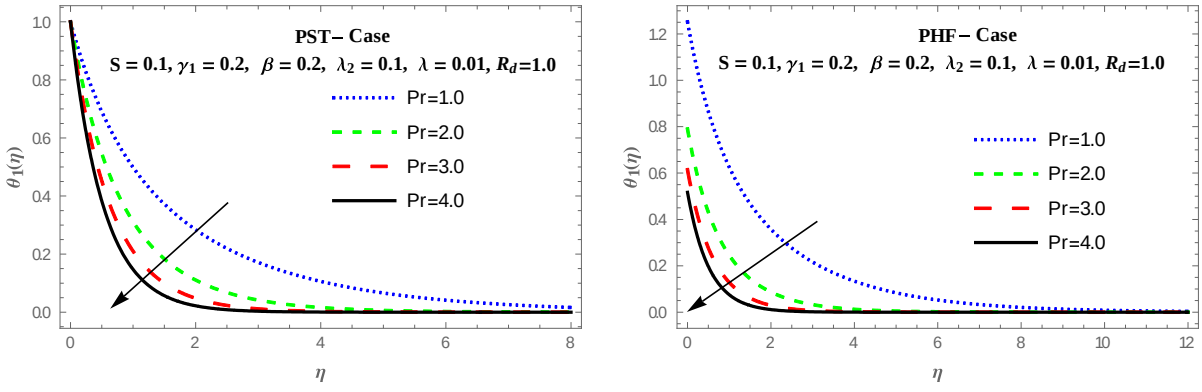

(a) (b)

Fig. 11. Influence of Prandtl number Pr on temperature θ_1: (a) for PST and (b) for PHF

How the radiation parameter R_d acts on the velocity of the fluid is presented for the PST and PHF cases in Figure 12(a) and Figure 12(b). It is observed that for each value of R_d the velocity decreases as we move from point zero on the sheet toward infinity. However, increasing the values of R_d does not bring about much significant change. The temperature distribution in both processes PST and PHF is shown in Figure 13(a) and Figure 13(b), where we see that as R_d rises the temperature also rises. This is because thermal radiation causes the thermal boundary layer thickness to increase. Therefore, for the rate of the fluid's cooling process to be faster radiation has to be considerably reduced.

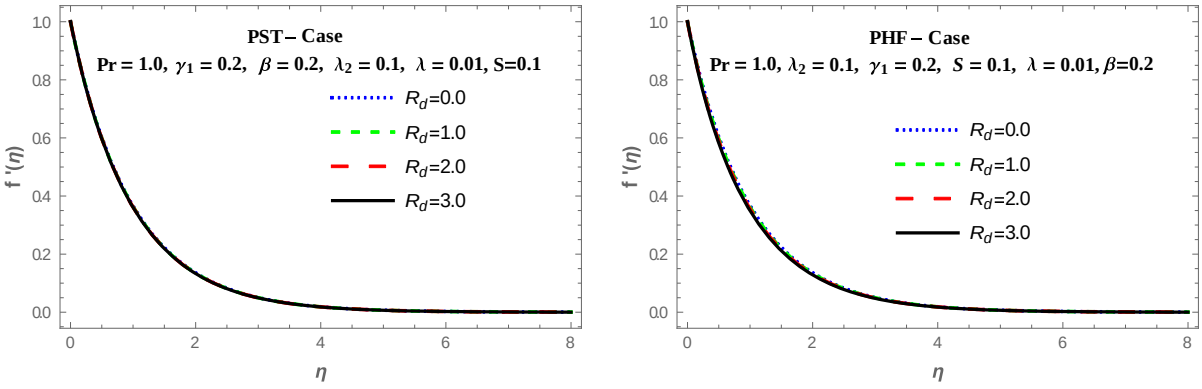

(a) (b)

Fig. 12. Influence of Radiation parameter R_d on velocity $f'(\eta)$: (a) for PST and (b) for PHF

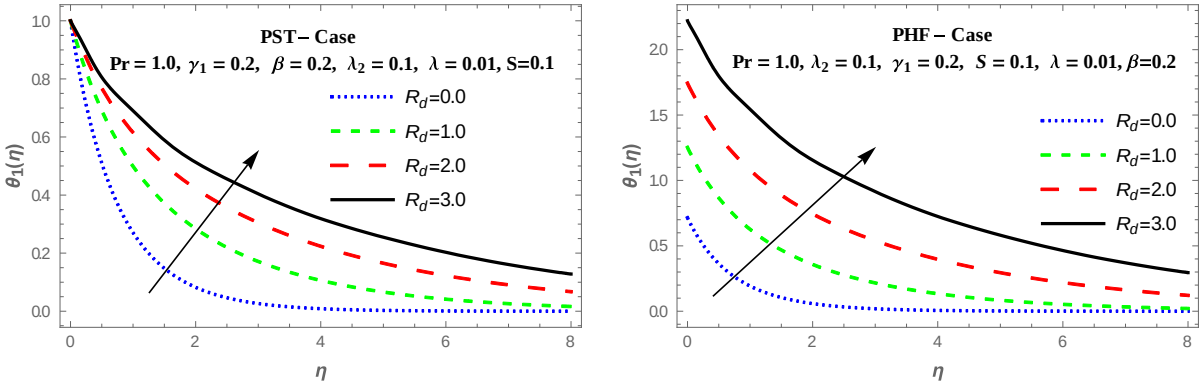

(a) (b)

Fig. 13. Influence of Radiation parameter R_d on temperature θ_1: (a) for PST and (b) for PHF

As can be seen in Figure 14, increasing values of the Prandtl number cause a reduction in the skin friction coefficient as the value of the ferromagnetic interaction parameter increases. In Figure 15, it is observed that for increasing positive values of S there is an increase in the skin friction coefficient as the value of β is less than two (2); but the reverse is the case for the skin friction coefficient when the value of β is greater than two (2). These are in agreement with Zeeshan and Majeed [1] as we had set the value of the radiation parameter to zero.

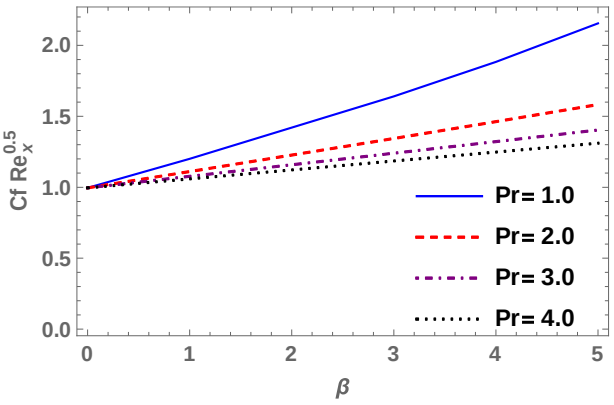

Fig. 14. Skin friction coefficient with variation in ferromagnetic interaction parameter for different values of Prandtl number, when radiation parameter is zero

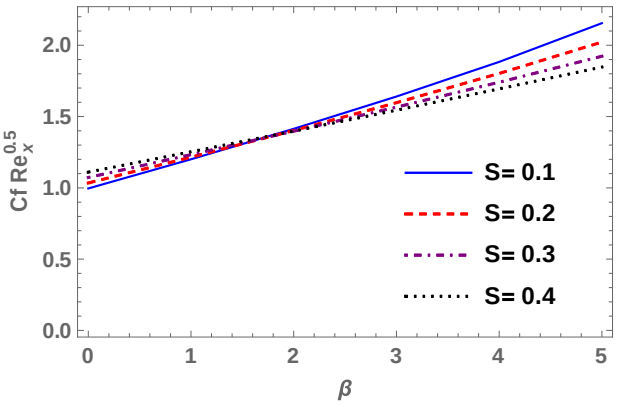

Fig. 15. Skin friction coefficient with variation in ferromagnetic interaction parameter for different values of Suction/injection parameter, when radiation parameter is zero

4. Conclusions

We have considered the flow and heat transfer of a Jeffery fluid past a stretching sheet under the influence of thermal radiation and magnetic dipole for both the prescribed surface temperature (PST) and prescribed heat flux (PHF) heating processes. Using the Chebyshev spectral collocation method to solve the governing equations we obtained solutions for the velocity and temperature which were compared to the result obtained by the Generic algorithm (GA) and Neader Mead (NM) method of Zeeshan and Majeed [1] when thermal radiation was not present ($R_d = 0$), and there was a very good agreement. The behavior of the velocity and temperature when we varied the different parameters present in the model was illustrated by the use of graphs and provided extensive explanations for each of them. Below are pertinent results as determined by this research work

i. Thermal radiation parameter brings about an increase in temperature for both PST and PHF heating processes.
ii. The effect of the magnetic dipole as depicted by the ferromagnetic interaction parameter on the velocity of the flow is a reduction, while it steadily increases temperature for the

PST case but there is a dual effect of increment and reduction of temperature for the PHF case.

iii. The Deborah number (γ_1) increases fluid velocity and reduces the temperature for both heating processes.

iv. The ratio of relaxation to retardation time parameter λ_2 reduces velocity and results in a temperature rise.

v. The suction/injection parameter S causes a fall in both the velocity and temperature of the fluid.

Acknowledgment
This research was not funded by any grant.

References

[1] Zeeshan, A., and A. Majeed. "Heat transfer analysis of Jeffery fluid flow over a stretching sheet with suction/injection and magnetic dipole effect." *Alexandria Engineering Journal* 55, no. 3 (2016): 2171-2181. https://doi.org/10.1016/j.aej.2016.06.014

[2] Sakiadis, Byron C. "Boundary-layer behavior on continuous solid surfaces: I. Boundary-layer equations for two-dimensional and axisymmetric flow." *AIChE Journal* 7, no. 1 (1961): 26-28. https://doi.org/10.1002/aic.690070108

[3] Crane, Lawrence J. "Flow past a stretching plate." *Zeitschrift für angewandte Mathematik und Physik ZAMP* 21 (1970): 645-647. https://doi.org/10.1007/BF01587695

[4] Gupta, P. S., and A. S. Gupta. "Heat and mass transfer on a stretching sheet with suction or blowing." *The Canadian Journal of Chemical Engineering* 55, no. 6 (1977): 744-746. https://doi.org/10.1002/cjce.5450550619

[5] Ariel, P. Donald. "Extended homotopy perturbation method and computation of flow past a stretching sheet." *Computers & Mathematics with Applications* 58, no. 11-12 (2009): 2402-2409. https://doi.org/10.1016/j.camwa.2009.03.013

[6] Chakrabarti, A., and A. S. Gupta. "Hydromagnetic flow and heat transfer over a stretching sheet." *Quarterly of Applied Mathematics* 37, no. 1 (1979): 73-78. https://doi.org/10.1090/qam/99636

[7] Chen, C-H. "Laminar mixed convection adjacent to vertical, continuously stretching sheets." *Heat and Mass transfer* 33 (1998): 471-476. https://doi.org/10.1007/s002310050217

[8] Ishak, Anuar, Khamisah Jafar, Roslinda Nazar, and Ioan Pop. "MHD stagnation point flow towards a stretching sheet." *Physica A: Statistical Mechanics and Its Applications* 388, no. 17 (2009): 3377-3383. https://doi.org/10.1016/j.physa.2009.05.026

[9] Narayana, PV Satya, and D. Harish Babu. "Numerical study of MHD heat and mass transfer of a Jeffrey fluid over a stretching sheet with chemical reaction and thermal radiation." *Journal of the Taiwan Institute of Chemical Engineers* 59 (2016): 18-25. https://doi.org/10.1016/j.jtice.2015.07.014

[10] Xu, Hang, and Shi-Jun Liao. "Laminar flow and heat transfer in the boundary-layer of non-Newtonian fluids over a stretching flat sheet." *Computers & Mathematics with Applications* 57, no. 9 (2009): 1425-1431. https://doi.org/10.1016/j.camwa.2009.01.029

[11] Zeeshan, A., and A. Majeed. "Non Darcy mixed convection flow of magnetic fluid over a permeable stretching sheet with ohmic dissipation." *Journal of Magnetics* 21, no. 1 (2016): 153-158. https://doi.org/10.4283/JMAG.2016.21.1.153

[12] Akinbo, B. J. "Influence of Convective Boundary Condition on heat and mass transfer in a Walters' B fluid over a vertical stretching surface with thermal-diffusion effect." *Journal of Thermal Engineering* 7, no. 7 (2021): 1784-1796. https://doi.org/10.18186/thermal.1026001

[13] Akinbo, B. J., and B. I. Olajuwon. "Radiation and thermal-diffusion interaction on stagnation-point flow of Walters' B fluid toward a vertical stretching sheet." *International Communications in Heat and Mass Transfer* 126 (2021): 105471. https://doi.org/10.1016/j.icheatmasstransfer.2021.105471

[14] Akinbo, Bayo Johnson, and Bakai Ishola Olajuwon. "Heat transfer analysis in a hydromagnetic Walters' B fluid with elastic deformation and Newtonian heating." *Heat Transfer* 50, no. 3 (2021): 2033-2048. https://doi.org/10.1002/htj.21967

[15] Akinbo, B. J., B. I. Olajuwon, I. A. Osinuga, and S. I. Kuye. "Effect of Chemical Reaction and Thermo-Diffusion in an Electrically Conducting Walters' B Fluid over a Vertical Stretching Surface Effect of Chemical Reaction and Thermo-Diffusion in an Electrically Conducting Walters' B Fluid over a Vertical Stretching Surface." *TECNICA ITALIANA-Italian Journal of Engineering Science* 65, no. 1 (2021): 36-44. https://doi.org/10.18280/ti-ijes.650106

[16] Akinbo, B. J., and B. I. Olajuwon. "Impact of radiation and chemical reaction on stagnation-point flow of Hydromagnetic Walters' B fluid with Newtonian heating." *International Communications in Heat and Mass Transfer* 121 (2021): 105115. https://doi.org/10.1016/j.icheatmasstransfer.2021.105115
[17] Akaje, T. W., and B. I. Olajuwon. "Effects Of Inclined Magnetic Field And Slip Boundary Condition On Heat And Mass Transfer In A Casson Nanofluid Flow Over A Stretching Sheet." *Journal of Sciences & Technology* 5, no. 1 (2020): 15-28.
[18] Akaje, Wasiu Toyin. "Stagnation point heat flow and mass transfer in a Casson nanofluid with viscous dissipation and inclined magnetic field." *UKH Journal of Science and Engineering* 5, no. 1 (2021): 38-49. https://doi.org/10.25079/ukhjse.v5n1y2021.pp38-49
[19] Akaje, Wasiu, and B. I. Olajuwon. "Impacts of Nonlinear thermal radiation on a stagnation point of an aligned MHD Casson nanofluid flow with Thompson and Troian slip boundary condition." *Journal of Advanced Research in Experimental Fluid Mechanics and Heat Transfer* 6, no. 1 (2021): 1-15.
[20] Dalir, Nemat. "Numerical study of entropy generation for forced convection flow and heat transfer of a Jeffrey fluid over a stretching sheet." *Alexandria Engineering Journal* 53, no. 4 (2014): 769-778. https://doi.org/10.1016/j.aej.2014.08.005
[21] Hayat, Tasawar, Muhammad Waqas, Sabir Ali Shehzad, and Ahmed Alsaedi. "MHD stagnation point flow of Jeffrey fluid by a radially stretching surface with viscous dissipation and Joule heating." *Journal of Hydrology and Hydromechanics* 63, no. 4 (2015): 311-317. https://doi.org/10.1515/johh-2015-0038
[22] Sandeep, Naramgari, Chalavadi Sulochana, and Isaac Lare Animasaun. "Stagnation-point flow of a Jeffrey nanofluid over a stretching surface with induced magnetic field and chemical reaction." In *International Journal of Engineering Research in Africa*, vol. 20, pp. 93-111. Trans Tech Publications Ltd, 2016. https://doi.org/10.4028/www.scientific.net/JERA.20.93
[23] Hayat, Tasawar, and Meraj Mustafa. "Influence of thermal radiation on the unsteady mixed convection flow of a Jeffrey fluid over a stretching sheet." *Zeitschrift für Naturforschung A* 65, no. 8-9 (2010): 711-719. https://doi.org/10.1515/zna-2010-8-913
[24] Raju, C. S. K., N. Sandeep, and Machireddy Gnaneswara Reddy. "Effect of nonlinear thermal radiation on 3D Jeffrey fluid flow in the presence of homogeneous-heterogeneous reactions." In *International Journal of Engineering Research in Africa*, vol. 21, pp. 52-68. Trans Tech Publications Ltd, 2016. https://doi.org/10.4028/www.scientific.net/JERA.21.52
[25] Hayat, T., R. Sajjad, and S. Asghar. "Series solution for MHD channel flow of a Jeffery fluid." *Communications in Nonlinear Science and Numerical Simulation* 15, no. 9 (2010): 2400-2406. https://doi.org/10.1016/j.cnsns.2009.09.033
[26] Animasaun, I. L., C. S. K. Raju, and N. Sandeep. "Unequal diffusivities case of homogeneous-heterogeneous reactions within viscoelastic fluid flow in the presence of induced magnetic-field and nonlinear thermal radiation." *Alexandria Engineering Journal* 55, no. 2 (2016): 1595-1606. https://doi.org/10.1016/j.aej.2016.01.018
[27] Shehzad, Sabir Ali, Tasawar Hayat, Ahmed Alsaedi, and Mustafa Ali Obid. "Nonlinear thermal radiation in three-dimensional flow of Jeffrey nanofluid: a model for solar energy." *Applied Mathematics and Computation* 248 (2014): 273-286. https://doi.org/10.1016/j.amc.2014.09.091
[28] Das, Kalidas, Nilangshu Acharya, and Prabir Kumar Kundu. "Radiative flow of MHD Jeffrey fluid past a stretching sheet with surface slip and melting heat transfer." *Alexandria Engineering Journal* 54, no. 4 (2015): 815-821. https://doi.org/10.1016/j.aej.2015.06.008
[29] Dalir, Nemat, Mohammad Dehsara, and S. Salman Nourazar. "Entropy analysis for magnetohydrodynamic flow and heat transfer of a Jeffrey nanofluid over a stretching sheet." *Energy* 79 (2015): 351-362. https://doi.org/10.1016/j.energy.2014.11.021
[30] Hayat, T., Gulnaz Bashir, M. Waqas, and A. Alsaedi. "MHD flow of Jeffrey liquid due to a nonlinear radially stretched sheet in presence of Newtonian heating." *Results in Physics* 6 (2016): 817-823. https://doi.org/10.1016/j.rinp.2016.10.001
[31] Narayana, Mahesha, L. S. Rani Titus, Annamma Abraham, and Precious Sibanda. "Modelling micropolar ferromagnetic fluid flow due to stretching of an elastic sheet." *Afrika Matematika* 25 (2014): 667-679. https://doi.org/10.1007/s13370-013-0145-7
[32] Andersson, H. I., and O. A. Valnes. "Flow of a heated ferrofluid over a stretching sheet in the presence of a magnetic dipole." *Acta Mechanica* 128, no. 1-2 (1998): 39-47. https://doi.org/10.1007/BF01463158
[33] Titus, L. S. Rani, and A. Abraham. "Ferromagnetic Liquid Flow due to Gravity-Aligned Stretching of an Elastic Sheet." *Journal of Applied Fluid Mechanics* 8, no. 3 (2015): 591-600. https://doi.org/10.18869/acadpub.jafm.67.222.21973
[34] Nadeem, Sohail, and Noreen Sher Akbar. "Peristaltic flow of a Jeffrey fluid with variable viscosity in an asymmetric channel." *Zeitschrift für Naturforschung A* 64, no. 11 (2009): 713-722. https://doi.org/10.1515/zna-2009-1107

[35] Raptis, A. "Flow of a micropolar fluid past a continuously moving plate by the presence of radiation." *International Journal of Heat and Mass Transfer* 18, no. 41 (1998): 2865-2866. https://doi.org/10.1016/S0017-9310(98)00006-4
[36] Pruett, C. David, and Craig L. Streett. "A spectral collocation method for compressible, non-similar boundary layers." *International Journal for Numerical Methods in Fluids* 13, no. 6 (1991): 713-737. https://doi.org/10.1002/fld.1650130605
[37] Sobamowo, M. G., L. O. Jayesimi, and M. A. Waheed. "Chebyshev Spectral Collocation Method for Flow and Heat Transfer in Magnetohydrodynamic Dissipative Carreau Nanofluid over a Stretching Sheet with Internal Heat Generation." *AUT Journal of Mechanical Engineering* 3, no. 1 (2019): 3-14. https://doi.org/10.14529/jcem190101
[38] Abel, M. Subhas, Emmanuel Sanjayanand, and Mahantesh M. Nandeppanavar. "Viscoelastic MHD flow and heat transfer over a stretching sheet with viscous and ohmic dissipations." *Communications in Nonlinear Science and Numerical Simulation* 13, no. 9 (2008): 1808-1821. https://doi.org/10.1016/j.cnsns.2007.04.007
[39] Khan, Ansab Azam, Khairy Zaimi, Suliadi Firdaus Sufahani, and Mohammad Ferdows. "MHD flow and heat transfer of double stratified micropolar fluid over a vertical permeable shrinking/stretching sheet with chemical reaction and heat source." *Journal of Advanced Research in Applied Sciences and Engineering Technology* 21, no. 1 (2020): 1-14. https://doi.org/10.37934/araset.21.1.114
[40] Rehman, Fouzia, Muhammad Imran Khan, Muhammad Sadiq, and Asad Malook. "MHD flow of carbon in micropolar nanofluid with convective heat transfer in the rotating frame." *Journal of Molecular Liquids* 231 (2017): 353-363. https://doi.org/10.1016/j.molliq.2017.02.022
[41] Khan, Muhammad Ijaz, Siraj Ullah, Tasawar Hayat, Muhammad Waqas, Muhammad Imran Khan, and Ahmed Alsaedi. "Salient aspects of entropy generation optimization in mixed convection nanomaterial flow." *International Journal of Heat and Mass Transfer* 126 (2018): 1337-1346. https://doi.org/10.1016/j.ijheatmasstransfer.2018.05.168
[42] Rusdi, Nadia Diana Mohd, Siti Suzilliana Putri Mohamed Isa, Norihan Md Arifin, and Norfifah Bachok. "Thermal Radiation in Nanofluid Penetrable Flow Bounded with Partial Slip Condition." *CFD Letters* 13, no. 8 (2021): 32-44. https://doi.org/10.37934/cfdl.13.8.3244
[43] Kotnurkar, Asha S., and Namrata Kallolikar. "Effect of Surface Roughness and Induced Magnetic Field on Electro-Osmosis Peristaltic Flow of Eyring Powell Nanofluid in a Tapered Asymmetric Channel." *Journal of Advanced Research in Numerical Heat Transfer* 10, no. 1 (2022): 20-37.
[44] Bailey, R. L. "Lesser known applications of ferrofluids." *Journal of Magnetism and Magnetic Materials* 39, no. 1-2 (1983): 178-182. https://doi.org/10.1016/0304-8853(83)90428-6